

Evaluation of biocathodes in freshwater and brackish sediment microbial fuel cells

Liesje De Schamphelaire · Pascal Boeckx ·
Willy Verstraete

Received: 11 March 2010 / Revised: 20 April 2010 / Accepted: 21 April 2010 / Published online: 14 May 2010
© Springer-Verlag 2010

Abstract Biofilms on biocathodes can catalyze the cathodic oxygen reduction and accordingly guarantee high cathode redox potentials. The present research assessed the use of biocathodes in full-sediment microbial fuel cells. Carbon felt-based biocathodes were evaluated in freshwater systems, and an extension of their application to brackish systems and/or stainless steel webs as base material was considered. Efficient biocathodes could be developed within days through inoculation with active microorganisms. Carbon felt was found most suited for the biocathodes in freshwater with increased performance at salinities around 80–250 mM. Maximum long-term performance reached $12.3 \mu\text{W cm}^{-2}$ cathode. The relative benefit of stainless steel seemed to increase with increasing salinity. A combination of stainless steel cathodes with biofilms could, however, also result in decreased electrical performance. In an efficiently catalyzing cathodic biofilm, an enrichment with an uncultured *Proteobacterium*—previously correlated with steel waste—was observed.

Keywords Biocathode · Carbon · Stainless steel · Sediment microbial fuel cell

Electronic supplementary material The online version of this article (doi:10.1007/s00253-010-2645-9) contains supplementary material, which is available to authorized users.

L. De Schamphelaire · W. Verstraete (✉)
Laboratory of Microbial Ecology and Technology (LabMET),
Ghent University,
Coupure Links 653,
9000 Gent, Belgium
e-mail: Willy.Verstraete@UGent.be

P. Boeckx
Laboratory of Applied Physical Chemistry (ISOFYS),
Ghent University,
Coupure Links 653,
9000 Gent, Belgium

Introduction

Sediment microbial fuel cells (SMFCs) are bacterial batteries in which reduced (in)organic compounds are (microbially) oxidized at an anode buried in the sediment layer and where the final electron acceptor is reduced at the cathode, positioned in the overlying water layer. They are an adaptation of reactor-type MFCs, where anode and cathode are contained in one or two closed compartments, mostly separated by a membrane. In MFC research, biological reactions at the cathode have long been the secondary point of interest. The topic is however gaining interest, with an increasing number of biologically catalyzed cathode reactions being developed and/or studied, for instance involving manganese or nitrate (He and Angenent 2006). Cathodic oxygen reduction reactions have formed an essential part of “abiotic” marine fuel cells (Wilcock and Kauffman 1997), but it was not until recently that the biological aspect of these reactions became the focus of attention. Biocorrosion—being the underlying principle for these reactions—forms the basis of the present biocathode research, where a biocathode is defined as a cathode using microorganisms to assist in cathodic reactions. Bergel et al. (2005) hence developed a stainless steel cathode for a marine fuel cell, where a biofilm on the cathode led to a 100-fold increase in power density.

At several instances in literature, biocathodes have been shown to be good alternatives (Clauwaert et al. 2007; De Schamphelaire et al. 2008; Rabaey et al. 2008) or upgrades (Bergel et al. 2005; Faimali et al. 2008) compared to chemical cathodes for use in (microbial) fuel cells. Their use is especially advantageous in the sediment MFC, which is open to the environment, implying exposure to catalyst poisoning compounds and continuous renewal of the “cathodic liquid.”

Graphite and carbon have conventionally been used as electrode material in MFCs. Only few papers deal with O₂-reducing biocathodes from carbon or graphite and this in reactor-type MFCs [e.g., Clauwaert et al. (2007), Rabaey et al. (2008)]. Lately, there are several reports regarding electroactive biofilms on stainless steel plates and this in marine waters, mainly without a corresponding bioanode [e.g. Bergel et al. (2005), Erable et al. (2010), and Faimali et al. (2008)]. In the present research a highly performing non-polarized biocathode, originally developed with carbon felt in a freshwater SMFC and deployed in our earlier experiments (De Schamphelaire et al. 2008), was further characterized on electrochemical and molecular basis in full SMFCs (involving a biocathode and bioanode) and evaluated for extended use to brackish systems and/or with stainless steel web as electrode material.

Materials and methods

Reactors with set salinity

Two cylindrical reactors of 22.5 cm in diameter were filled with 10 cm (4 L) of potting soil [Structural Professional type 1, M. Snebbout N.V., Kaprijke, Belgium; peat based, enriched with NPK (nitrogen–phosphorus–potassium) fertilizer 14–16–18 at 1.25 kg m⁻³, 150 mg SO₄²⁻L⁻¹, 20% organics, pH5–6.5] and a 10-cm water layer. One reactor was operated as freshwater reactor (reactor F, with tapwater), while the other one was operated as brackish water reactor (reactor B, tapwater with added NaCl), by precedingly stepwise increasing the salinity up to about 200 mM. Each sediment layer contained two anodes of carbon felt (Sigratherm KFA, SGL Carbon Group, Germany, 5 mm thickness) of 6.5×7.5 cm [geometric

area (GA) of 49 cm²], while four cathodes were submerged in the overlying water layer (see also Table 1). Two cathodes were made from carbon felt (C) (2.5 mm thick) and two from stainless steel (SS) (316L, web from fibers of 2 or 8 μm diameter, Bekaert, Belgium). One SS cathode and one C cathode were operated in closed circuit with the two anodes, with an external resistance of 500 Ω, while the other two cathodes were left in open circuit. Anodes and cathodes were interwoven with a graphite rod (Morgan, 5 mm diameter), which was attached to the electrical circuitry through an insulated connection (anodes) or a clamp (cathodes). Water layers were sparged with air, unless otherwise mentioned. Aliquots of water from previously operated SMFCs with biocathodes were used as cathode inoculum. This was originally obtained by inoculating a cathode with several types of sediments, soil, river water, sludge, and manganese-oxidizing strains.

Several series of new cathode sets were applied in the reactors through time, with the operating parameters shown in Table 1. The reactors were placed either in a greenhouse with variable temperature or a laboratory at room temperature. Pieces of cathodes were cut off at the indicated time points for subsequent molecular analysis. Where indicated in Table 1, the cathodic surface was brought to 11.5 cm² GA before polarization curves were recorded (1–2 weeks in advance). During all polarizations, new (i.e., without biofilm) premoistened cathodes of equal sizes were analyzed for comparison. Values for pH of water layers varied between 7.7 and 8.5, with the pH of reactor B 0.2–0.5 pH units lower than of reactor F.

Setups with varying salinity

Smaller types of SMFCs were constructed in order to vary salinity. These cells had a surface of 11×11 cm. They were

Table 1 Overview of the parameters characterizing the different series of cathodes deployed in freshwater (F) and brackish water (B, 200 mM NaCl) systems

Series	Time period (mm/yy–mm/yy)	Place	Temperature (min/max–min/max or mean±SD, in °C)	Type of reactor	Cathode material and original size (GA)	DGGE sampling (months after startup)	Operational parameters during polarization curves (months after startup, type of reactor, cathode GA)
1	03/08–06/08	GH	19/34–21/44	F+B	C+8 μm SS, 36 cm ²	1.5	–
2	07/08–09/08	GH	21/46–23/42	F+B	C+2 μm SS, 36 cm ²	–	–
3	09/08–10/08	GH	23/42–22/39	F+B	C+2 μm SS, 36 cm ²	–	–
4	10/08–01/09	GH	22/39–18/30	F+B	C+2 μm SS, 36 cm ²	1.5, 3	1.75, F, B, 11.5 cm ²
5	01/09–07/09	GH	18/30–22/47	F	C+2 μm SS, 17 cm ²	–	4.5–5, F, 17 cm ²
	07/09–09/09	Lab	22±2	F→B	C+2 μm SS, 17 cm ²	–	7, F, 17 cm ² ; 8, B, 17 cm ² ; 8.5, B, 11.5 cm ²
6	08/09–09/09	Lab	22±2	B	C+2 μm SS, 17 cm ²	–	1.5, B, 11.5 cm ²

About 7–7.5 months after startup of series 5, the salinity of reactor F was gradually increased by adding NaCl
GH greenhouse, Lab laboratory, C carbon felt, SS stainless steel, SD standard deviation, GA geometric area

filled with 4.5 cm (0.5 L) of potting soil and 8 cm (1 L) of tap water. In order to change the salinity, the overlying water layer was removed by siphoning and gently replaced by tap water to which NaCl was added. After diffusion, this process was repeated until a desired salinity was obtained. The salinity was hence increased from 0 mM (overlying tapwater, 0.73 mS cm^{-1} , referred to as 0 mM or freshwater) to maximum 700 mM in steps of about 100 mM over a period of 10 months. The resulting salinity was verified by measuring conductivity (Consort C833, electrode SK20T, Belgium) and recalculating it to salinity. Carbon felt anodes (Sigratherm KFA, SGL Carbon Group, Germany, 5 mm thickness) of $6 \times 9 \text{ cm}$ (GA of 54 cm^2) were placed at the bottom of each sediment layer. Two SMFCs (cells C1 and C2) contained a carbon felt cathode (Alfa Aesar, USA, 3 mm thickness), while two (cells SS1 and SS2) contained a stainless steel cathode (316L, web, 8 μm fibers, Bekaert, Belgium), all of which were $5 \times 12.5 \text{ cm}$ (GA of 62.5 cm^2). Electrical connections and inoculation were performed as described for the previous setup. Reactors were operated at room temperature, and water layers were continuously sparged with air, pH was 7.9 ± 0.1 .

Electrochemical parameters and analysis

All SMFCs were operated with an external resistance of 500Ω . Cell and redox potentials were measured and recorded every 1, 15, or 20 min (Agilent HP 34970A). Calculations were performed according to Logan et al. (2006). Electrical current and power density refer to cathodic geometric surface areas (GA) at all times. Values for ohmic losses were determined through the current interrupt method based on the potential jump after 0.2 ms. Polarization curves were imposed and recorded with a BiStat-2-channel potentiostat (BioLogic Science Instruments, France) with the anode as working electrode and the cathode as counter electrode. Cells were allowed to reach open circuit potential during 2 h, after which the cell potential was continuously varied (rate of 1 or 0.05 mV s^{-1}) or stepwise varied (about ten steps of 20 min divided equally over the cell potential range). The Ag/AgCl reference electrode (BASi, model RE-5B, UK or ORION 900200 Double Junction, Thermo Scientific, USA) was positioned near the cathode in order to measure the cathode redox potential. Anode redox potentials were approximated by subtracting cell potential from cathode redox potentials.

Molecular analysis

Total DNA of 2 g (for SS cathodes) or 4 g (for thicker C cathodes) of wet cathode material or 2 mL of aqueous solution was extracted using standard methods (Boon et al. 2002) and purified (Wizard[®] DNA Clean-Up System,

Promega). Bacterial 16S rRNA gene fragments were amplified with primers PRBA338fGC and P518r (Muyzer et al. 1993), and PCR products were analyzed by denaturing gradient gel electrophoresis (DGGE) (gradient from 45% to 60%, 16 h at 38 V) (Boon et al. 2002). Gel patterns were normalized and analyzed using Bionumerics 5.1 (Applied Maths).

For phylogenetic analysis, bands of interest were excised from DGGE gels as described before (Aelterman et al. 2006). After amplification (without GC clamp) and purification (with Qiagen PCR Purification Kit), the product was submitted to IIT Biotech (Germany) for sequencing. Sequences were manually checked using Chromas 2.33 and aligned with sequences from GenBank with the BLAST server (NCBI, April 2010) or analyzed using Ribosomal Database Project (Wang et al. 2007). Sequences referring to bands 1–4 were deposited with GenBank under accession numbers GU129135–GU129138.

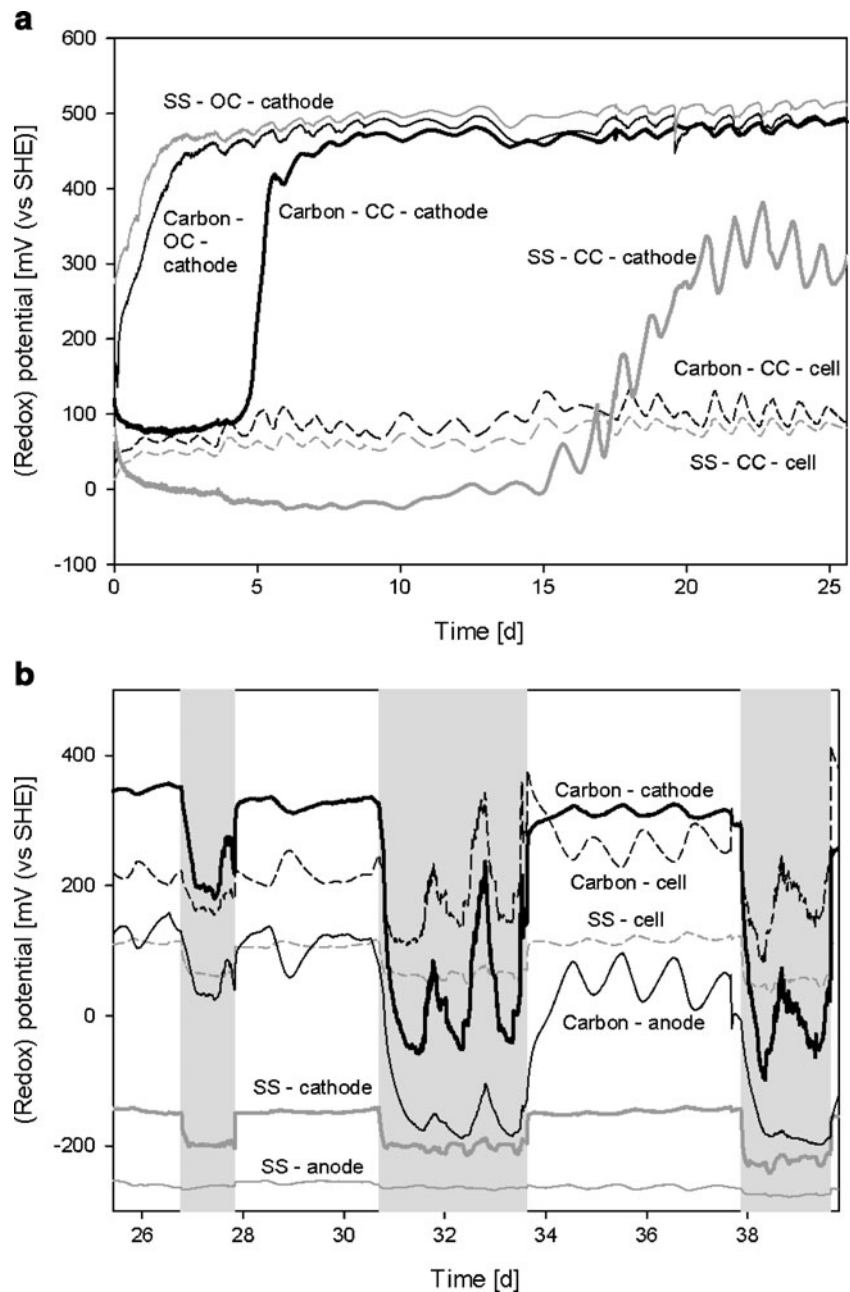
Results

Reactors with set salinity: overall performance

Several subsequent series of cathodes, with different operational conditions, were started in lab-scale sediment systems, of which the water layer was inoculated with the performant electrocatalytic biofilm. During startup, the cathode redox potentials demonstrated a characteristic sigmoidal course (see Fig. 1a and Fig. S1a in the Online Resource). The redox potential of carbon felt (C) and stainless steel (SS) cathodes operated in open circuit reached comparable high values around 400–450 mV vs. standard hydrogen electrode (SHE) within 1–3.5 days, which is an increase of 200 mV or more. When operated in closed circuit, it took the C cathodes 3–8 days to reach high redox potentials (at the same level). The rise in redox potential was accompanied by a slight to strong (Fig. S1a) increase in cell potential, depending on the series. Longer lag periods (about 20 days) were required for the redox potential increase to take place in case of SS cathodes and lower values (350 mV vs. SHE or lower) were reached. Moreover, in some SS series, the increase could not even be observed after 2.5 months.

Cell potentials and hence current and power obtained with the C cathodes were also higher than those obtained with the SS cathodes. Anodes were switched several times per reactor to ascertain that differences were not due to inherent differences in anode performance. With each anode combination, the electrical production was equal and even higher (up to factor 10) for the C cathodes than for the SS cathodes (e.g. 3.9 ± 1.7 vs. $0.24 \pm 0.14 \mu\text{W cm}^{-2}$

Fig. 1 Details of performance during reactor run. **a** Cell potential (mV) during cathode startup in freshwater sediment–water systems (reactor F, series 1, early spring). **b** Cell potential (in mV) and redox potential of electrodes (in mV vs. SHE) during an alternating aeration–non-aeration experiment in a freshwater sediment–water system with closed circuit biocathodes (reactor F, series 3, late summer). Periods during which no aeration was applied to the water surrounding the cathode are shaded. *Black* Carbon felt cathodes, *gray* stainless steel (SS) cathodes, *dashed lines* closed circuit cell potential (CC-cell), *bold full lines* cathode redox potential in closed circuit (CC-cathode), *thin full lines*: cathode redox potential in open circuit (OC-cathode) for **a** and anode redox potential in closed circuit (anode) for **b**



for reactor F, series 5, greenhouse). Average current densities obtained with the cathodes in all series varied between 5 and 26 $\mu\text{A cm}^{-2}$ for C cathodes in freshwater, 4 and 7 $\mu\text{A cm}^{-2}$ for SS cathodes in freshwater, 5 and 12 $\mu\text{A cm}^{-2}$ for C cathodes in brackish water, and 3 and 5 $\mu\text{A cm}^{-2}$ for SS cathodes in brackish water, with the higher values obtained in warmer periods. No clear differences between SS with 2 and 8 μm fibers could be observed. The ohmic losses were $66 \pm 10 \Omega$ for the C–freshwater system, $91 \pm 23 \Omega$ for the SS–freshwater system, $6.9 \pm 3.7 \Omega$ for the C–brackish water system, and $5.7 \pm 3.1 \Omega$ for the SS–brackish water system.

Reactors with set salinity: effect of aeration

The influence of aeration, and hence the supply of the final electron donor, was evaluated through alternating aeration–non-aeration cycles of the water surrounding the cathode (see Fig. 1b and Fig. S1b). The redox and cell potentials of the SS cathode dropped significantly when the aeration was stopped. For the C cathode system, these drops were either more or less pronounced, depending on the level of the cell potential at the onset of the test. The potential fluctuations were superimposed on diurnal fluctuations.

Reactors with set salinity: polarization curves

Several runs of polarization curves were performed on cathodes that had been operated in closed or open circuit for a substantial time and on newly installed cathodes. A representative selection of results can be found in Figs. 2 and 3. Table S1 in the Online Resource presents a second set of results as well as averages over several test series. Absolute values could vary considerably between the test series. The trends among the different types of cathode were however similar, except where mentioned otherwise.

Freshwater–carbon felt cathodes In the freshwater system, the cells with a closed circuit (CC) carbon felt cathode performed clearly better than with an open circuit (OC) cathode, i.e., when the cathode was present in the same fluid, but had not been electrically connected before (Fig 2a, Table S1): the maximum power production was a factor 1.5–4 higher. The OC carbon cathode at its turn performed comparably better than a newly prepared carbon

cathode. No clear trend could be observed regarding the maximum current output. Overall, absolute maxima of $94 \mu\text{A cm}^{-2}$ and $28 \mu\text{W cm}^{-2}$ were obtained with carbon felt cathodes. The two types of “mature” carbon cathodes had comparable open circuit potentials (OCP) (up to 722 mV) and corresponding OC redox potentials (up to 548 mV vs. SHE); both were about 200 mV higher than for a new carbon cathode. The well operating CC carbon cathode demonstrated a lower slope in the cathode redox potential decrease upon current increase. Maximum electrical performance occurred at higher cathode redox potentials (about 300 mV vs. SHE) compared to OC cathodes (about 210 mV vs. SHE) and especially compared to new cathodes (about -20 mV vs. SHE).

Freshwater –stainless steel web cathodes Also for SS cathodes, operated in the same freshwater system, the OCP values with CC and OC cathodes were significantly higher than those with newly installed SS cathodes. The difference was 125–300 mV, as was the

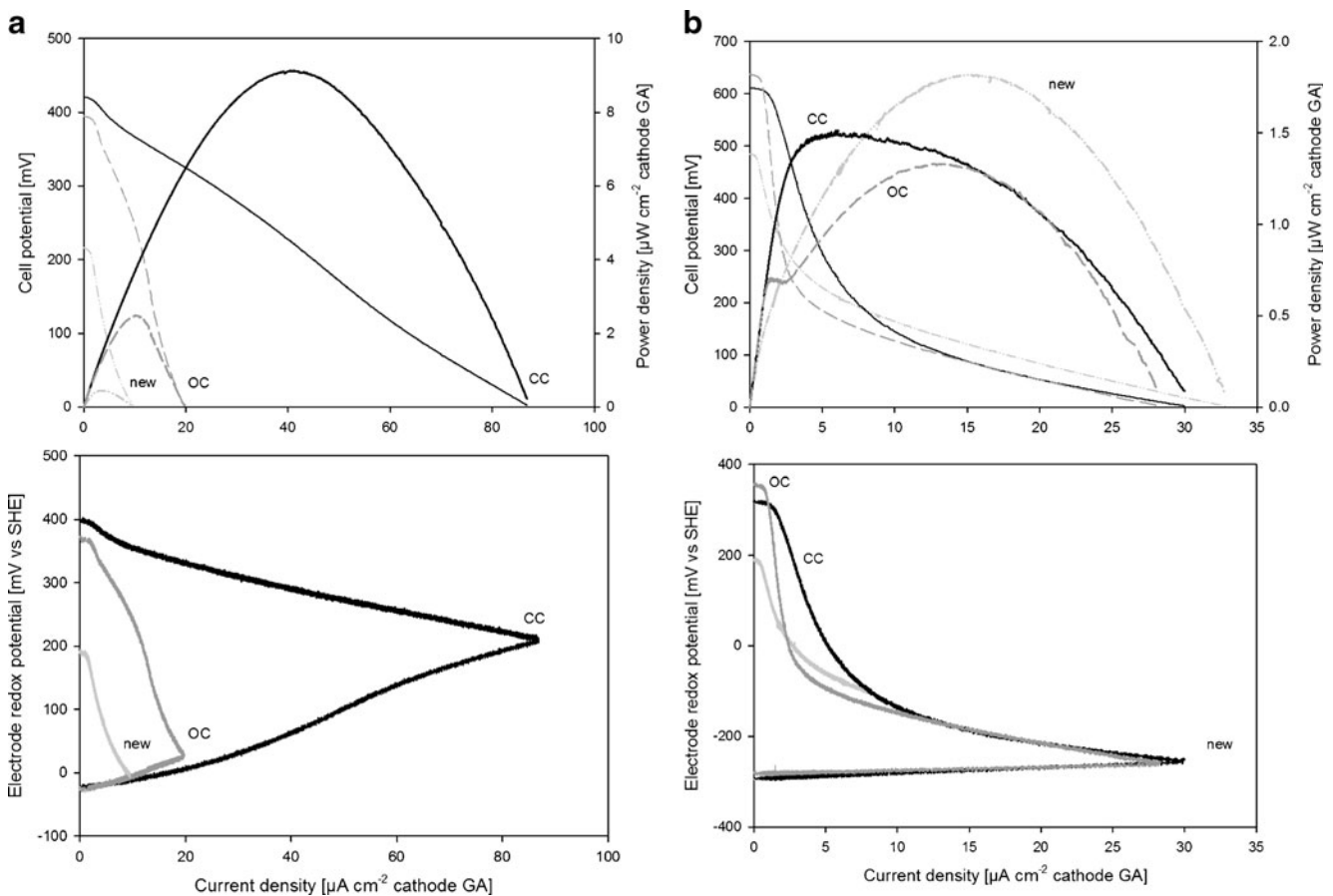


Fig. 2 Polarization curves for several types of **a** carbon felt and **b** stainless steel cathodes operated within a freshwater system (reactor F, series 4, greenhouse, begin winter, $11.5 \text{ cm}^2 \text{ GA}$). Polarization curves are successively represented by cell potential (*thin lines*) and power density curves (*bold lines*) and by electrode redox potential curves

(the cathode redox potential is the upper part of two divergent curves). *Full black lines* Cathodes that had been operated in closed circuit (CC), *dashed dark gray lines* cathodes that had been operated in open circuit (OC), *dash-dotted light gray lines* newly deployed cathodes. Scan rate 1 mV s^{-1}

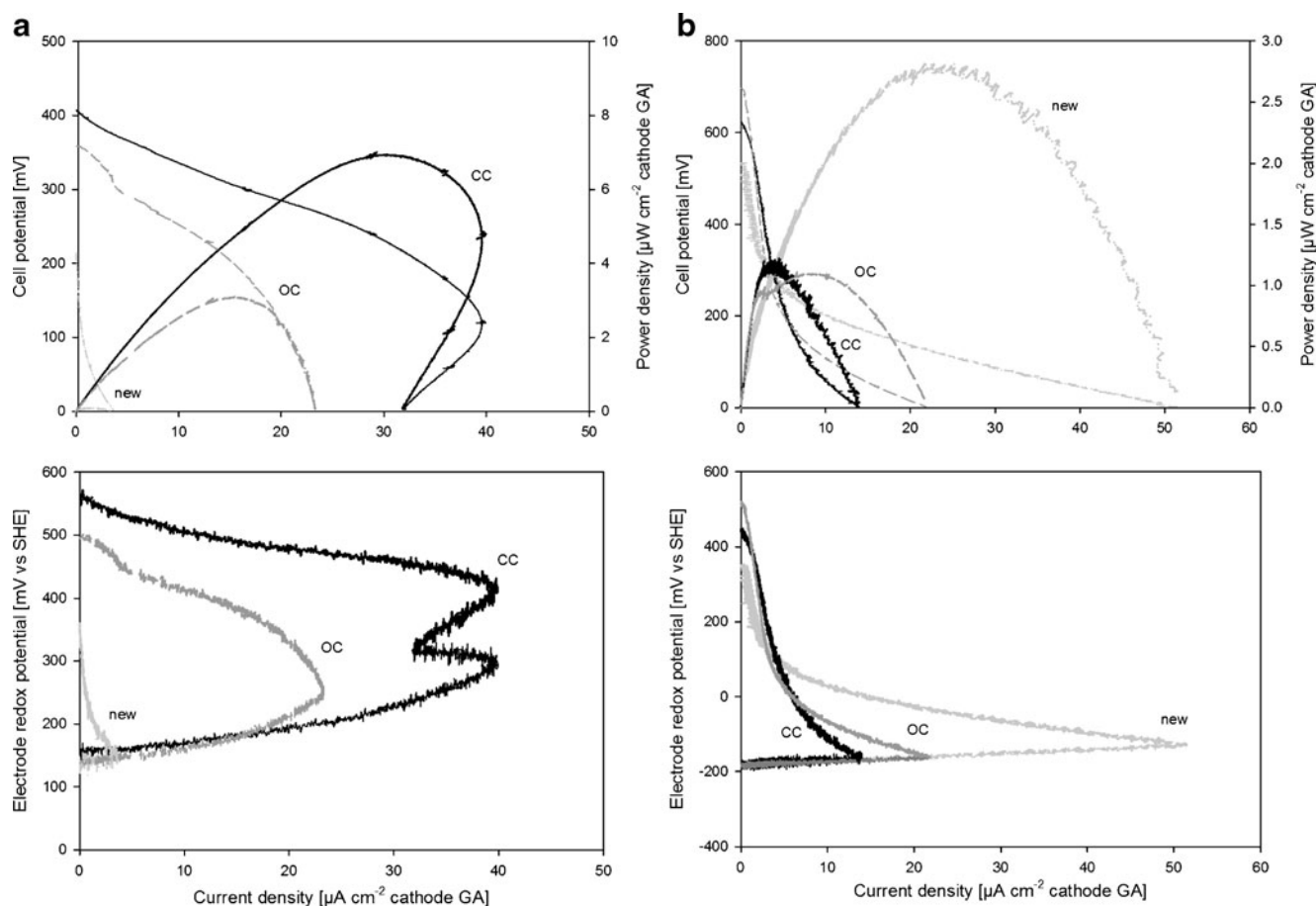


Fig. 3 Polarization curves for several types of **a** carbon felt and **b** stainless steel cathodes operated within a brackish sediment–water system (reactor B, series 5, Lab, 11.5 cm² GA). Polarization curves are successively represented by cell potential (*thin lines*) and power density curves (*bold lines*) and by electrode redox potential curves

(the cathode redox potential is the upper part of two divergent curves). *Full black lines* Cathodes that had been operated in closed circuit (CC), *dashed dark gray lines* cathodes that had been operated in open circuit (OC), *dash-dotted light gray lines* newly deployed cathodes. Scan rate, 1 mV s⁻¹

case with the cathode redox potentials at OCP (Fig. 2b, Table S1). Absolute values could differ and could get up to 705 mV for OCP and 545 mV vs. SHE for the open circuit cathode redox potential. Cathode potentials showed a rapid decline during polarization curves down to values of -268 mV vs. SHE. However, CC and OC cathodes often reached high cathode potentials (around 300 mV vs. SHE) at maximum power, as opposed to the low to negative values with new cathodes. Remarkably, power production was comparable or (slightly) higher (factors 1–4) for new cathodes than for OC or CC cathodes, while the latter two were more equal. New cathodes also reached higher maximum current densities than CC or OC cathodes (factors 1–4). Absolute maxima obtained with SS cathodes were 36 $\mu\text{A cm}^{-2}$ and 2 $\mu\text{W cm}^{-2}$.

Brackish water–carbon felt cathodes In reactor B, the attainable production could be either lower, of comparable

level, or higher than in reactor F, depending on the test series. Absolute performance maxima recorded with C cathodes in the brackish system were 0.17 mA cm⁻² and 20 $\mu\text{W cm}^{-2}$. In general, CC cathodes performed better than OC cathodes, which at their turn performed better than new cathodes (Fig. 3a, Table S1). OCP values and corresponding cathode potentials were about 140–200 mV higher for the mature cathodes than for a new cathode. The cathode redox potentials of CC cathodes showed a lower decline during polarization than in case of new cathodes.

Brackish water–stainless steel web cathodes When SS cathodes were applied in the brackish system, the results were comparable or higher than those with SS in freshwater. However, trends among the different types of cathodes differed significantly throughout the test series. For example, in series 4, the OC cathode performed best (about 1.75 months after

startup), while in series 5, the new cathode performed best (8 months after startup) (Fig. 3b). These variable trends indicate that the cathodic cover (biofilm and/or precipitates) can have a positive as well as a negative effect on performance. Absolute performance maxima obtained with SS cathodes in the brackish system were $37 \mu\text{A cm}^{-2}$ and $5 \mu\text{W cm}^{-2}$. Despite the different trends, the OCP as well as the corresponding cathode potential were always higher (about 150–300 mV) for the OC cathodes than for new cathodes, with the CC cathodes having an intermediate value. Steep cathode potential declines were recorded for all polarization curves; CC cathodes generally demonstrated the highest (often positive) redox potentials at maximum power.

The polarization curves, which were shown and discussed so far, were based on a potentiodynamic rate of 1 mV s^{-1} . Curves were also recorded at lower rates (0.05 mV s^{-1} and stepwise), resulting in the same trends but lower absolute performance values. At some instances (at high as well as low rate), limitation phenomena occurred, such as intermediate maxima (e.g. Fig. 2b, begin of OC power curve) or bending back of current (e.g. Fig. 3a, CC, from cell potentials lower than 120 mV).

Reactors with set salinity: molecular analysis

At three time points during the different series in reactors F and B, samples of cathode material plus biofilm were cut for subsequent molecular analysis. Cluster analyses of the obtained DGGE profiles showed that the composition of the biofilm on cathode surfaces differed from that of suspended microorganisms and that the cathodic biofilms from the brackish systems were substantially different from those of the freshwater systems (Fig. 4). Within one system, the type of material could either have a stronger (Fig. 4a, c) or a smaller effect (Fig. 4b) than the type of electrical circuit.

Several bands were cut from the DGGE gels and successfully sequenced. Band 1 was especially present in the water surrounding the cathodes and could with 100% certainty be classified as *Pseudomonas*. Band 2 appeared under various but mostly OC conditions. It could, with 97% certainty, be classified as *Ralstonia*. Band 3 occurred in varying DGGE profiles but was highly enriched on a CC carbon felt cathode in freshwater, while this was not the case with the corresponding OC cathode. This band could with 97% certainty be classified with *Proteobacteria* (86% for γ -*Proteobacteria*) and was 100% similar with uncultured γ -*Proteobacteria* clones from steel plant waste [EU447521–EU447524 and EU447527 (Freitas et al. 2008)] and an uncultured bacterium clone from a reactor treating groundwater contaminated with nitrate and uranium (DQ202169). Band 4 was especially enriched on cathodes from the brackish water reactor and likely represents a key member of the dense

grey-greenish biofilm, which had overall developed in the brackish system. It could, with 92% certainty, be classified with *Cyanobacteria*.

Setups with varying salinity

In another type of setup, each SMFC was installed in a separate reactor, of which the salinity was stepwise increased. The results shown in Fig. 5 originate from one set of cells (cells C1 and SS1). The trends observed with the duplicate set (cells C2 and SS2), shown in Table S2 in the Online Resource, were analogous.

Carbon felt cathodes with varying salinity Stepwise recorded polarization curves for cell C1 (Fig. 5a) showed that the electrical performance increased upon increasing salinity with high performance around 80–230 mM, after which the performance declined. This was the case for maximum power density, maximum current density, and maximum cell potential. Cathode redox potentials were highly positive, only slightly decreased (30–50 mV) upon current density increase and were barely influenced by salinity. The effect of salinity on the anode redox potential was however more pronounced. Salinity furthermore decreased the ohmic losses, with a drop from $91 \pm 37 \Omega$ at 0 mM to $13 \pm 5 \Omega$ at 80 mM, after which the ohmic losses slightly decreased/remained rather equal. Maximum current and power densities obtained with continuous polarization (Fig. S2a in the Online Resource) were a factor 4 higher, but the same trends were observed, with best performance at 80 mM. For cell C2 (Table S2), best performances at stepwise polarization were also obtained in the 100–250 mM range. Long-term currents produced by both cells (at 500Ω) also reached higher values at intermediate salinity. Overall, an average current of $1.6 \pm 0.5 \mu\text{A cm}^{-2}$ was obtained with both carbon felt cathodes.

Stainless steel web cathodes with varying salinity The performance with SS cathodes demonstrated the same trends as with C cathodes upon increasing salinity (intermediate maximum, stepwise polarization in Fig. 5b), although the trend in OCP was only minor. OCP values were about double to triple of those with C cathodes. Optimal performance was reached around a salinity of 340 mM. With SS cathodes, the decrease in cathode potential was much steeper than the increase in anode potential, but the slope was less steep at higher salinities. Ohmic losses decreased from $108 \pm 46 \Omega$ at 0 mM to $13 \pm 4 \Omega$ at 80 mM, after which the ohmic losses only slightly decreased. Maximum current and power densities obtained with continuous polarization (Fig. S2b) followed the same trends but were about a factor 2 higher. The values and trends of cell SS2 were analogous (Table S2), although power density could be double of that of cell SS1 and the best

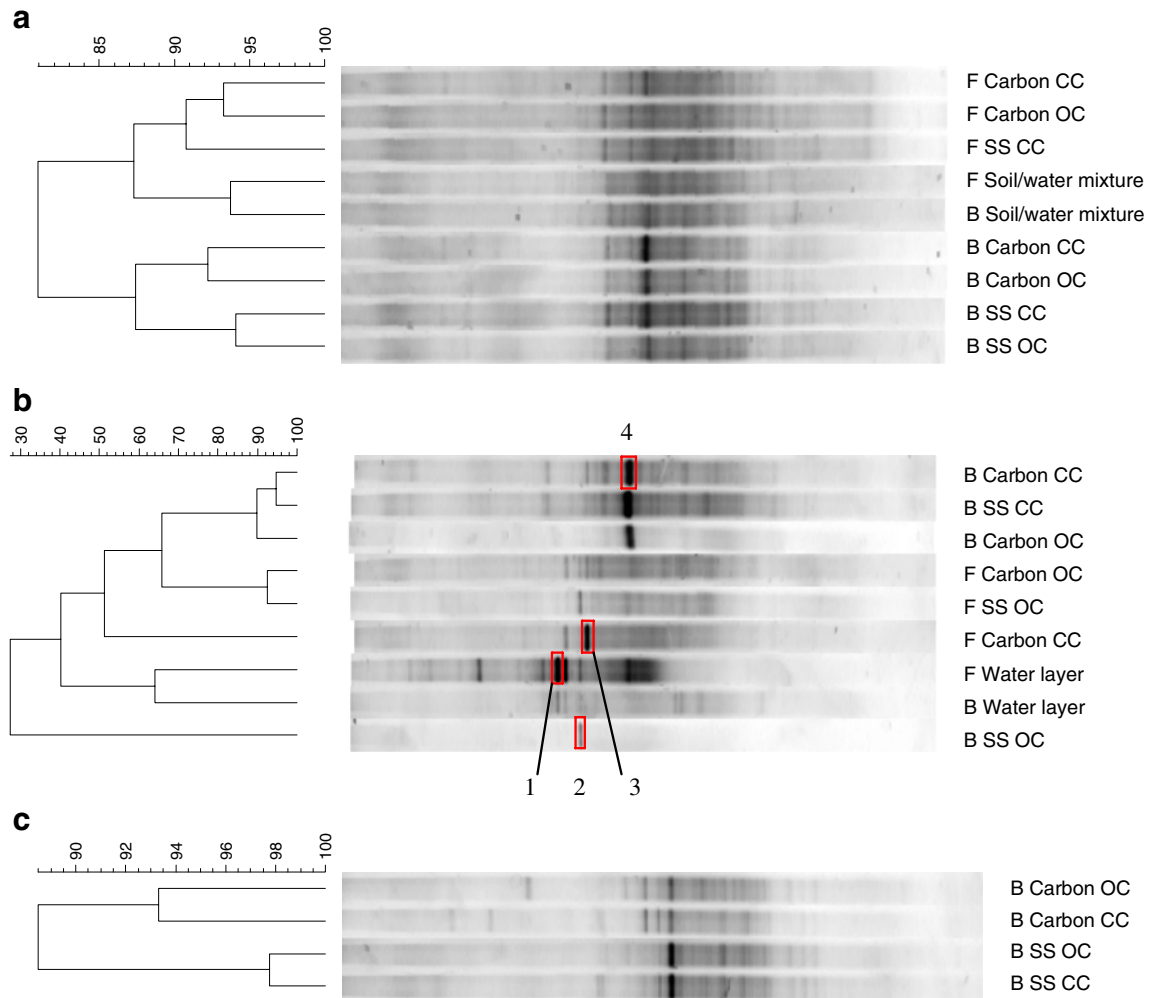


Fig. 4 Cluster analysis of cathode and soil/water samples from reactor F (freshwater) and reactor B (brackish) cut off during **a** series 1, after 1.5 months of operation, **b** series 4, after about 1.5 months and **c** series 4, after about 3 months. *Carbon* Carbon felt, *SS* stainless steel webs,

CC closed circuit operation, *OC* open circuit operation. Cluster analyses were performed according to Pearson's correlation and the UPGMA algorithm. Excised DGGE bands are indicated with *numbers 1–4*

performance was reached around 110–320 mM. The long-term current density (at 500 Ω) of both reactors reached an average of $1.3 \pm 0.5 \mu\text{A cm}^{-2}$, which is slightly lower than that of the C cathodes. The same trend as before was observed.

Discussion

General performance of the primary freshwater–carbon-based biocathode

The freshwater deployed carbon felt biocathodes reached long-term (order of months) current and power densities of $2.0 \pm 0.5 \mu\text{A cm}^{-2}$ and $0.1 \pm 0.2 \mu\text{W cm}^{-2}$ in case the anode

was about 15% smaller in size than the cathode (cells C1–C2, lab at room temperature). However, when the cathode was only about one third of the surface area of the anode, the obtained sustained electrical densities could be at least a factor 10 higher: $22 \pm 4 \mu\text{A cm}^{-2}$ and $4.2 \pm 1.5 \mu\text{W cm}^{-2}$ (reactor F, series 5, greenhouse, February to April). This indicates that the cathodic reaction had a high efficiency and that the anode was probably the limiting factor in these systems. The latter could be due to slower kinetics as well as lower mass transfer of substrate to the anode. It should be mentioned that the oxygen mass transfer to the cathode was increased through air sparging. The higher cathodic than anodic efficiency was reflected in the lower slope of the cathode redox potential versus current density (see e.g. Fig 3a). Still higher outputs could be obtained in series 3

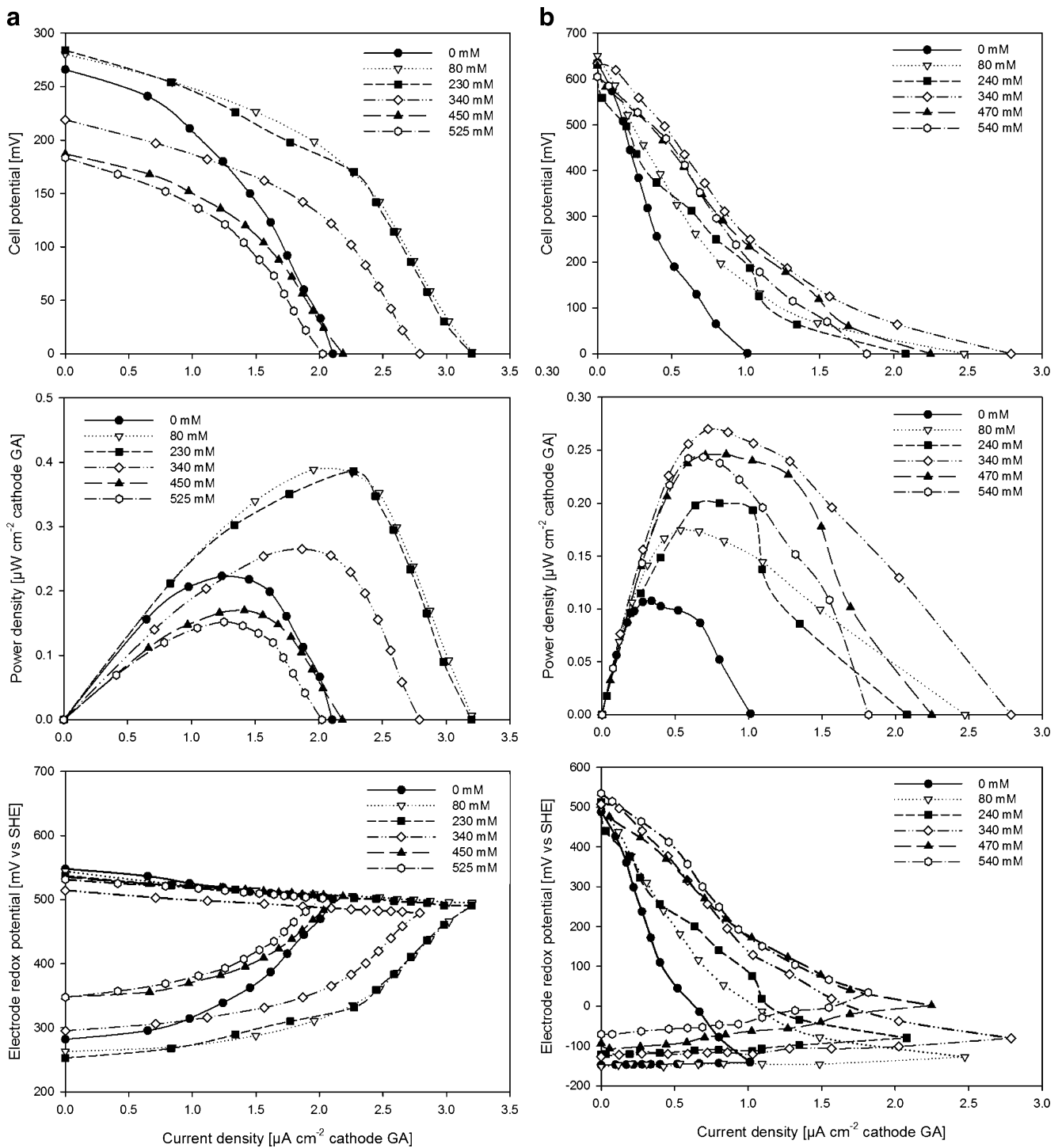


Fig. 5 Stepwise polarization curves under varying salinity for a carbon felt cathodes (cell C1) and b stainless steel cathodes (cell SS1). Polarization curves are successively represented by cell potential

curves, power density curves, and electrode redox potential curves. The cathode redox potential is the upper part of two divergent curves. All cathodes were operated in closed circuit between polarizations

with reactor F (greenhouse, September, anode 35% larger than cathode), namely $26 \pm 2 \mu\text{A cm}^{-2}$ and $12 \pm 1 \mu\text{W cm}^{-2}$ (corresponding with 123 mW m^{-2} or 1.23 kW ha^{-1}), likely due to higher temperature. The obtained cathodic reaction rates are still lower than those obtained with biocathodes in

reactor-type MFCs, which reached values up to $270 \mu\text{A cm}^{-2}$ and $90 \mu\text{W cm}^{-2}$ in continuous mode (Clauwaert et al. 2007), but this is expected to be due to overall lower internal resistance (reactor configuration, electrode geometries, and medium composition) of a

reactor-type MFC. Maximum obtainable performance by the present sediment MFC biocathodes, as determined through polarization curves (1 mV s^{-1}) at room temperature, reached values of $94 \mu\text{A cm}^{-2}$ and $20 \mu\text{W cm}^{-2}$. The specific effect of cathode material and salinity will be discussed in the following sections. Overall, during the recording of some polarization curves, limitations in the system could be observed, for instance through a bending back of the cell potential curve (Fig. 3a; no steady increase in current density). A similar observation was made by Aelterman et al. (2006), and it was dedicated to mass transfer limitations.

Onset of biocathode catalysis

The onset of efficient cathode catalysis was observed through a sigmoidal increase in cathode redox potential (termed ennoblement), accompanied by a slight to strong sigmoidal increase in cell potential and hence current density (see Fig. 1a). The magnitude of the latter increase was likely related to the operational temperature as the increases were stronger in warmer periods. Whereas the redox potential increase for closed circuit cathodes took several weeks in earlier non-reported experiments, the onset could here be shortened to 3 days. This was accomplished by deploying the cathodes in closed systems where the necessary microorganisms were already present through the start and/or operation of previous biocathodes, without polarization required. Inoculation hence clearly promotes the development of electrocatalytic biofilms and is an advantageous strategy to adopt during the assemblage of SMFCs.

Within MFC research, such a sigmoidal pattern in closed or open circuit cathode redox potential (Reimers et al. 2006) or current density (Dumas et al. 2007) has been previously observed in marine systems. Others found a sigmoidal increase in current density indicating biocathode startup upon cathodically polarizing SS cathodes (i.e., actively decreasing the redox potential) to values of for instance 0 mV vs. SHE (Bergel et al. 2005). It should however be noticed that a cathodic biofilm developed in the latter way will be adapted to low redox potentials, while high positive redox potentials are warranted for fuel cell conditions, in which electrical current is spontaneously produced.

The sigmoidal increase in cathodic current has been found proportional to the number of settled bacteria (Faimali et al. 2008). Indeed, when such a cathodic biofilm was removed (Bergel et al. 2005) or killed through autoclaving (Clauwaert et al. 2007), cathodic performance decreased significantly. In the present case, the performance of cathodes, which had been operating in closed or open circuit for several weeks, was compared to that of newly

deployed cathodes, without biofilm (Fig. 2a). The biofilm resulted in a tenfold increase in performance (reactor F, carbon cathode, closed circuit).

A biofilm-induced increase in (cathode) redox potential is often observed on (metal) alloys. It is found related to metal corrosion, but the underlying mechanism is not yet completely understood. It has been suggested to involve, among others, (1) decreased pH, following the Nernst equation, (2) enzymes, increasing the exchange current, (3) the production of H_2O_2 , and (4) the precipitation of MnOx , the latter two both resulting in zones and reactions with high redox potential (Little et al. 2008), and/or (5) the consumption of the protective H_2 layer through for instance nitrate reduction (Kielemoes et al. 2000b). In the present case, the ennoblement can, additionally, be regarded with respect to oxygen reduction, in which the biofilm is presumed to act as a catalyst (Rabaey et al. 2008).

The biofilm as a catalyst for cathodic oxygen reduction

Oxygen has poor reduction kinetics at a cathode in MFC conditions (Zhao et al. 2006). Strategies to improve the oxygen cathode reaction involve the use of chemical catalysts (Logan et al. 2006), enzymes (Schaeztle et al. 2009), and high cathode surface areas (Freguia et al. 2007). A biofilm can also act as catalyst for oxygen reduction. It namely has a higher affinity for oxygen than cathode material as such [critical dissolved oxygen concentration of 1 mg L^{-1} for an aerobic bacterial culture vs. $6.6 \text{ mg O}_2\text{L}^{-1}$ for graphite (Pham et al. 2004)]. Furthermore, a biofilm can enhance the electron transfer rate to oxygen (Bergel et al. 2005).

The redox potential at the cathode is ideally determined by the four electron reduction of oxygen ($E^{\circ'}=0.814 \text{ V vs. SHE}$). The redox potential will decrease with decreasing oxygen concentrations (according to the Nernst equation), through potential losses (activation, ohmic and concentration overpotential) and due to mixed potentials (because of other electron acceptors, incomplete reduction to H_2O_2). Through biofilm catalysis, the overall cathode overpotential will be decreased (Rabaey et al. 2008), to a large extent, because of lower activation losses. Decreased overpotentials result in higher redox potentials at higher current densities (see Fig. 2a). The role of the availability of oxygen as the final electron acceptor (cf. Nernst) was shown by intermittently stopping the sparging of the water layer, hence decreasing the supply of oxygen (Fig. 1b). Upon an oxygen decrease, there was a decrease in cathode redox potential and cell potential. This was especially the case when higher cell potentials and hence current densities were reached (Fig. 1b, carbon cell)—presumably because of higher temperatures—causing oxygen depletion to be a limiting factor. The biofilm catalysis was sufficient to

maintain a steady oxygen reduction rate (at high redox potential) at lower overall currents (Fig. S1b, carbon cell).

When applying the cathodes in the field, the energy consuming aeration can be circumvented by relying on forms of passive aeration (e.g., through high turbulence, rocks, small waterfalls, wind, and watermills), by applying for instance a rotating cathode (He et al. 2007) or by relying on photosynthetic activity.

The use of biofilms as catalyst entails a relatively low cost and assures a high sustainability compared to chemical catalysts (He and Angenent 2006), apart from a certain vulnerability caused by too low temperatures, fish grazing (Dumas et al. 2007), and loading with sediment material (Ryckelynck et al. 2005).

Molecular biofilm analysis

Through cluster analysis, it could be verified that the microbial communities growing in a biofilm on the cathodic surface had a different composition than those suspended in the water–sediment body. As the biofilms developing on SS were different from those developing on carbon, it could be assumed that the microbial members had different affinities for the materials. The salinity dependence of bacteria was reflected in the different community compositions in fresh and brackish situations. In some cases, a thick grey-greenish biofilm with presence of cyanobacteria had developed in the brackish system, as shown through sequencing. Phototrophic microorganisms (suspended or in a biofilm) can increase the oxygen delivery to the cathode and hence benefit the cathodic reaction rate (De Schamphelaire and Verstraete 2009), as long as biofilms do not become too thick and/or start internal decay.

The factor of electrical current production could also be deduced from the cathodic biofilm composition. For instance, in a freshwater system with carbon cathodes, an enrichment of the biofilm with an uncultured bacterium was apparent. The latter closely resembled several uncultured γ -*Proteobacteria* clones from a steelmaking waste dump (Freitas et al. 2008). It is plausible that this type of bacterium can shift from metal redox reactions to redox reactions with a solid electrode, as is the case with several members of the *Geobacteraceae* (Bond et al. 2002). This could imply that this bacterium is among the performant electroactive cathode bacteria and that SS materials or wastes can be a good source of inoculum for the development of both C- and SS-based biocathodes.

Other clear DGGE bands found in the cathode samples—however, not specific for closed circuit cathodes—could be classified as *Ralstonia* and *Pseudomonas*.

In previous research on biocathodes, in reactor-type as well as sediment-type MFCs, bacterial groups found to be

dominant on closed circuit anodes were α -, β -, γ - and δ -*Proteobacteria*, *Actinobacteria*, *Bacteroidetes*, and *Firmicutes* (Chen et al. 2008; Clauwaert et al. 2007; Holmes et al. 2004; Rabaey et al. 2008; Reimers et al. 2006). Most of that research however did not comprise a comparison with open circuit cathodes, whereas this was the case for the presently found γ -*Proteobacterium*-related species.

Effect of salinity

From the experiments (Fig. 5), it was clear that higher performances (twofold increase) were obtained in water with medium salinity (80–250 mM) than in freshwater. This follows from a higher conductivity and lower internal resistance of the system, as verified through the decreasing ohmic losses. Analogous observations were made in a reactor-type MFC by Liu et al. (2005). Salinities of 80–250 mM correspond with 0.47–1.44% salt, whereas seawater is at 3.5% salt. In the present case, the performance decreased again when the salinity reached high values, which can be explained by the salt sensitivity of bacterial species. Most halophobic freshwater microorganisms grow best in water with <1% salt (170 mM), although some freshwater bacteria can tolerate salinities of 2–4% (MacArthur 2006). The positive effect of salinity on electrical performance was larger for SS cathodes than for C cathodes. This might be related to the corrosion-promoting effect of chloride ions on SS (Little et al. 2008).

Although the present biocathode was originally developed for a freshwater sediment system, it clearly offers prospects for extended use in several types of inland or near-coast waters, where the performance might be further increased through inoculation/involvement of more halophilic microorganisms. This type of SMFC, which had a maximum long-term performance of $12 \mu\text{W cm}^{-2}$, can be a valid alternative to marine SMFCs, which reached sustainable outputs of 1.0 – $2.8 \mu\text{W cm}^{-2}$ (Ryckelynck et al. 2005) and non-sustainable values of $9.8 \mu\text{W cm}^{-2}$ (Lowy et al. 2006) (with anodes and cathodes of comparable size).

Cathode material

Throughout the experiments, the C-based cathodes revealed to be most effective, as higher current and power densities were obtained and overall, higher cathode potentials were maintained. The relative benefit of SS increased with increasing salinity. In previous comparative research in literature, both SS (Dumas et al. 2008) and carbon- or graphite-based material (Hasvold et al. 1997) have turned out to be most suited for cathode reactions, depending on the operational parameters.

In our tests, bare SS (without biofilm) performed better than bare C material. The sigmoidal increase in potential

however did not occur as easily in case of SS cathodes; furthermore, the maturation of the cathode sometimes had a negative effect on its performance (e.g., Fig. 3b). Biofilms can indeed have a negative effect on the cathode by creating anaerobic zones or by hindering the mass transfer of the electron acceptor, as previously observed by Tartakovsky and Guiof (2006). Electrochemical effects or precipitations as well as an overall different affinity of the bacteria for the materials might also be responsible for the limitation of the performance of SS as a cathode. Another possible explanation might be linked to the intrinsic nature of the cathode material. Stainless steel 316L contains relatively large amounts of Cr (16–18% by mass), Ni (10–14%) and Mo (2–3%) (Bekaert) for corrosion protection. These metals might, however, also have an effect on a microbial biofilm. Percival et al. (1998) and Kielemoes et al. (2000a) found a (slightly) lower colonisation of SS grade 316L than 304. This was attributed to a higher Mo content, which could leach out and decrease bacterial viability. In two distinct cooperative researches, the steel product company Bekaert (Belgium) recently found 316L to have anti-bacterial properties (Bekaert, personal communication). The high content of metals added to 316L could also have negatively affected the performance of the cathodic biofilm in the current research. A lower performance of a cathode with biofilm could, for instance, be related to oxygen consumption for the oxidation of died off biofilm. SS has been used in several previous researches on cathodic biofilms, often with even higher percentages of metal additives, but this mostly with plate material [for example in Bergel et al. (2005)]. In the present research, felt-like materials were chosen, consisting of a network of small fibers, having a low density (floatable) and a high actual surface. The latter however also means that a possible anti-bacterial effect will be more pronounced. Additionally, it can be mentioned that the thin, possibly smooth, fibers (2 or 8 μm in case of SS, about 10–20 μm in case of carbon felt) might have hampered the attachment of electroactive bacteria. However, it has been shown that bacteria can even attach to (assumingly smooth and unfavourable) fibers in perpendicular position (Rabaey et al. 2008). There were no consistent differences between SS material with 2 or 8 μm fibres.

Regarding the cathode material, it can finally be pointed out that despite non-optimal electrical performance of SS material, the latter still has better mechanical properties than carbon material concerning strength and cleaning (Hasvold et al. 1997).

In summary, biocathodes based on carbon material were found most suited for the operation of freshwater SMFCs, with even increased performance at medium salinity. The relative usefulness of stainless steel seemed to increase with salinity; however, its combination with a biofilm could also

negatively affect the cathodic performance. An efficiently operating cathodic biofilm can catalyze oxygen reduction and hence assures ennobled cathode redox potentials. Through inoculation with performant microorganisms (for instance bacteria related to steel waste), biocathodes can be started quickly, and biofilms can develop regardless of the operational conditions.

Acknowledgements LDS was supported through a PhD grant from the Bijzonder Onderzoeks Fonds of Ghent University (grant no. 01D24405). The useful comments of Nico Boon and Jan Arends are kindly acknowledged.

References

- Aelterman P, Rabaey K, Pham HT, Boon N, Verstraete W (2006) Continuous electricity generation at high voltages and currents using stacked microbial fuel cells. *Environ Sci Technol* 40:3388–3394
- Bergel A, Féron D, Mollica A (2005) Catalysis of oxygen reduction in PEM fuel cell by seawater biofilm. *Electrochem Commun* 7:900–904
- Bond DR, Holmes DE, Tender LM, Lovley DR (2002) Electrode-reducing microorganisms that harvest energy from marine sediments. *Science* 295:483–485
- Boon N, De Windt W, Verstraete W, Top EM (2002) Evaluation of nested PCR-DGGE (denaturing gradient gel electrophoresis) with group-specific 16 S rRNA primers for the analysis of bacterial communities from different wastewater treatment plants. *FEMS Microbiol Ecol* 39:101–112
- Chen GW, Choi SJ, Lee TH, Lee GY, Cha JH, Kim CW (2008) Application of biocathode in microbial fuel cells: cell performance and microbial community. *Appl Microbiol Biotechnol* 79:379–388
- Clauwaert P, Van der Ha D, Boon N, Verbeken K, Verhaege M, Rabaey K, Verstraete W (2007) Open air biocathode enables effective electricity generation with microbial fuel cells. *Environ Sci Technol* 41:7564–7569
- De Schampelaire L, Verstraete W (2009) Revival of the biological sunlight-to-biogas energy conversion system. *Biotechnol Bioeng* 103:296–304
- De Schampelaire L, van den Bossche L, Dang HS, Höfte M, Boon N, Rabaey K, Verstraete W (2008) Microbial fuel cells generating electricity from rhizodeposits of rice plants. *Environ Sci Technol* 42:3053–3058
- Dumas C, Basseguy R, Bergel A (2008) Microbial electrocatalysis with *Geobacter sulfurreducens* biofilm on stainless steel cathodes. *Electrochim Acta* 53:2494–2500
- Dumas C, Mollica A, Féron D, Basséguy R, Etcheverry L, Bergel A (2007) Marine microbial fuel cell: use of stainless steel electrodes as anode and cathode materials. *Electrochim Acta* 53:468–473
- Erable B, Vandecandelaere I, Faimali M, Delia M-L, Etcheverry L, Vandamme P, Bergel A (2010) Marine aerobic biofilm as biocathode catalyst. *Bioelectrochemistry* 78:51–56
- Faimali M, Chelossi E, Garaventa F, Corrà C, Greco G, Mollica A (2008) Evolution of oxygen reduction current and biofilm on stainless steels cathodically polarised in natural aerated seawater. *Electrochim Acta* 54:148–153
- Freguia S, Rabaey K, Yuan Z, Keller J (2007) Non-catalyzed cathodic oxygen reduction at graphite granules in microbial fuel cells. *Electrochim Acta* 53:598–603

- Freitas DB, Reis MP, Freitas LM, Assis PS, Chartone-Souza E, Nascimento AMA (2008) Molecular bacterial diversity and distribution in waste from a steel plant. *Can J Microbiol* 54:996–1005
- Hasvold O, Henriksen H, Melvaer E, Citi G, Johansen BO, Kjonigsen T, Galetti R (1997) Sea-water battery for subsea control systems. *J Power Sources* 65:253–261
- He Z, Angenent LT (2006) Application of bacterial biocathodes in microbial fuel cells. *Electroanal* 18:2009–2015
- He Z, Shao HB, Angenent LT (2007) Increased power production from a sediment microbial fuel cell with a rotating cathode. *Biosens Bioelectron* 22:3252–3255
- Holmes DE, Bond DR, O'Neill RA, Reimers CE, Tender LR, Lovley DR (2004) Microbial communities associated with electrodes harvesting electricity from a variety of aquatic sediments. *Microbiol Ecol* 48:178–190
- Kielemoes J, Hammes F, Verstraete W (2000a) Measurement of microbial colonisation of two types of stainless steel. *Environ Technol* 21:831–843
- Kielemoes J, De Boever P, Verstraete W (2000b) Influence of denitrification on the corrosion of iron and stainless steel powder. *Environ Sci Technol* 34:663–671
- Little BJ, Lee JS, Ray RI (2008) The influence of marine biofilms on corrosion: a concise review. *Electrochim Acta* 54:2–7
- Liu H, Cheng SA, Logan BE (2005) Power generation in fed-batch microbial fuel cells as a function of ionic strength, temperature, and reactor configuration. *Environ Sci Technol* 39:5488–5493
- Logan BE, Hamelers B, Rozendal R, Schröder U, Keller J, Freguia S, Aelterman P, Verstraete W, Rabaey K (2006) Microbial fuel cells: methodology and technology. *Environ Sci Technol* 40:5181–5192
- Lowy DA, Tender LM, Zeikus JG, Park DH, Lovley DR (2006) Harvesting energy from the marine sediment-water interface II - Kinetic activity of anode materials. *Biosens Bioelectron* 21:2058–2063
- MacArthur JV (2006) *Microbial ecology: an evolutionary approach*. Academic, Burlington
- Muyzer G, Dewaal EC, Uitterlinden AG (1993) Profiling of complex microbial populations by denaturing gradient gel electrophoresis analysis of polymerase chain reaction amplified genes coding for 16s ribosomal RNA. *Appl Environ Microbiol* 59:695–700
- Percival SL, Knapp JS, Edyvean RGJ, Wales DS (1998) Biofilms, mains water and stainless steel. *Water Res* 32:2187–2201
- Pham TH, Jang JK, Chang IS, Kim BH (2004) Improvement of cathode reaction of a mediatorless microbial fuel cell. *J Microbiol Biotechnol* 14:324–329
- Rabaey K, Read ST, Clauwaert P, Freguia S, Bond PL, Blackall LL, Keller J (2008) Cathodic oxygen reduction catalyzed by bacteria in microbial fuel cells. *ISME J* 2:519–527
- Reimers CE, Girguis P, Stecher HA, Tender LM, Ryckelynck N, Whaling P (2006) Microbial fuel cell energy from an ocean cold seep. *Geobiology* 4:123–136
- Ryckelynck N, Stecher HA, Reimers CE (2005) Understanding the anodic mechanism of a seafloor fuel cell: interactions between geochemistry and microbial activity. *Biogeochemistry* 76:113–139
- Schaetzle O, Barrière F, Schröder U (2009) An improved microbial fuel cell with laccase as the oxygen reduction catalyst. *Energy Environ Sci* 2:96–99
- Tartakovsky B, Guiot SR (2006) A comparison of air and hydrogen peroxide oxygenated microbial fuel cell reactors. *Biotechnol Prog* 22:241–246
- Wang Q, Garrity GM, Tiedje JM, Cole JR (2007) Naïve bayesian classifier for rapid assignment of rRNA sequences into the new bacterial taxonomy. *Appl Environ Microbiol* 73:5261–5267
- Wilcock WSD, Kauffman PC (1997) Development of a seawater battery for deep-water applications. *J Power Sources* 66:71–75
- Zhao F, Harnisch F, Schröder U, Scholz F, Bogdanoff P, Herrmann I (2006) Challenges and constraints of using oxygen cathodes in microbial fuel cells. *Environ Sci Technol* 40:5193–5199